Si:Au and Si:Pt $1S_{3/2}(\Gamma_8)+\Gamma$ phonon-assisted Fano resonance

M. Kleverman, J. Olajos, and P. Tidlund
Solid State Physics, University of Lund, Box 118, S-221 00 Lund, Sweden
(Received 21 January 1997; revised manuscript received 14 April 1997)

The excitation spectra for the Au and Pt acceptors in silicon have been studied by Fourier-transform infrared spectroscopy including uniaxial-stress perturbations. The resonancelike doublet structure, previously attributed to be the $2p'$ Coulombic line, is shown to be the $1S_{3/2}(\Gamma_8)$ phonon-assisted Fano resonance involving the zone-center Γ optical phonon. The deformation potentials b and d for the Au and Pt $1S_{3/2}(\Gamma_8)$ state are in good agreement with those previously determined for the B acceptor. Stress-induced preferential alignment effects are revealed for both centers. The doublet structure is shown to be due to crystal-field splitting of the $1S_{3/2}(\Gamma_8)$ Coulomb state. [S0163-1829(97)06428-X]

I. INTRODUCTION

The excitation spectrum of the Pt and the Au impurities in silicon are well known[1–3] and both are isolated substitutional defects with similar electronic structure.[4–6] For the neutral defects, the spectra are due to excitations from a deep ground state to shallowlike states in the band gap. Transitions to both shallow donor and acceptor states have been observed for Au but only the acceptor spectrum has been detected for Pt. Shallow acceptors in silicon have two sets of excited states bound by the Coulomb potential. The first set is found in the band gap and are denoted as the $P_{3/2}$ series since they are mainly derived from the upper $P_{3/2}$ valence band. A second set is mainly derived from the $P_{1/2}$ split-off band and transitions to p-like excited hole states, $nP_{1/2}$, have been observed for the shallow group-III acceptors. These lines are usually denoted $2p'$, $3p'$, ... in order of increasing excitation energy. The bound $nP_{1/2}$ states are resonant with the $P_{3/2}$ continuum and are discrete only in a zeroth-order approximation when neglecting the coupling between the discrete state and the valence-band continuum.

Several lines in the $P_{3/2}$ line series have been clearly resolved for both the Au and Pt acceptor.[2,3] The high-energy continuum part of the Au and the Pt acceptor spectra is presented in Fig. 1. Both the transmission and the photoconductivity (PC) spectra are shown for Pt whereas only the transmission spectrum for Au is reproduced in Fig. 1. F_1, F_2, and $F_{2'}$ denotes phonon-assisted Fano resonances (PAFR's), i.e., transitions to pseudodiscrete hole-phonon states that are resonant with the valence-band continuum. They consist[2,3] of the lowest $P_{3/2}$ acceptor states plus a Γ phonon (519 cm^{-1}). As is readily seen, the PAFR line shape varies considerably when observed in absorption compared to that for PC. This is a characteristic feature of PAFR's since in absorption all photons absorbed are also detected whereas in PC only those excited holes that finally enter the valence band contribute to the measured current.[7] As is also readily seen in Fig. 1 the PC result is more transparent since the resonance line shape is suppressed and the resonances are constituted of considerably sharper spectra features. This makes is easier to determine their energy positions although an inherent error comes from the unknown value of the Lamb shift.

A doublet structure, labeled $1S_{3/2}(\Gamma_8)+\Gamma$ in Fig. 1, was observed for both defects close to the energy position expected for the $2p'$ line which previously led us to tentatively assign it as the $2p'$ line for the two centers. This structure shows similar properties as the PAFR's in that the observed line shape is very different in absorption and PC. Also a second feature is observed labeled $1S_{3/2}(\Gamma_8)+\Gamma+\hbar\omega_{loc}$ in Fig. 1 and is a phonon replica of the $1S_{3/2}(\Gamma_8)+\Gamma$ line involving a Pt local phonon with an energy of about 58 cm^{-1}.[3] The labeling of the lines will become clear below. It was previously proposed[8] that the resonancelike line shape is due to a coupling between the $2p_{1/2}$ hole state and the

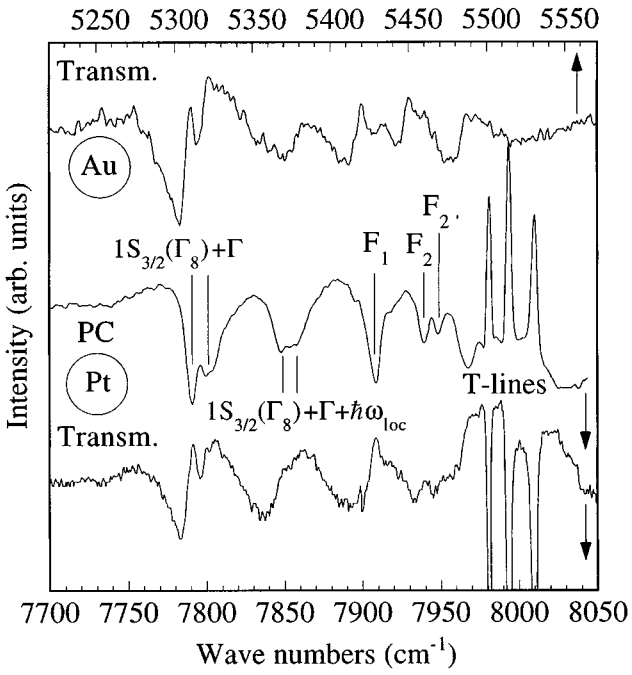

FIG. 1. Au (transmission) and Pt (transmission and photoconductivity) spectra showing the structures in valence-band continuum. F_1, F_2, and $F_{2'}$ indicate phonon-assisted Fano-resonances related to the $P_{3/2}$ series and the T lines (Ref. 18) are Pt-related donor lines. The $1S_{3/2}(\Gamma_8)+\Gamma$ doublet is the phonon-assisted Fano resonances involving the $1S_{3/2}(\Gamma_8)$ Coulombic acceptor state and the $1S_{3/2}(\Gamma_8)+\Gamma+\hbar\omega_{loc}$ doublet is the corresponding phonon replica involving a local phonon, $\hbar\omega_{loc}$ (see text for details).

valence-band continuum, i.e., a pure electronic Fano resonance. However, it was not possible in our previous work to explain why a doublet structure was observed. Various explanations were considered, e.g., chemical shifts and crystal-field splitting in the final-core state but all were necessarily rejected. It is well known that the $P_{3/2}$ excitation lines for the shallow group-III acceptors show chemical shifts, i.e., the various final states have impurity-dependent binding energies resulting in slightly different energy splitting between the lines for different centers.[9] The considerable delocalization of the $2p'$ and $3p'$ lines final states strongly indicates that the Au and Pt doublet structure is not due to a chemical shift that brings the $2p'$ and $3p'$ line closer in energy than observed for the group-III acceptors.

Both centers have a point-group symmetry that is lower than tetrahedral due to Jahn-Teller distortions. The negatively charged platinum center Pt has orthorhombic I symmetry[5] (C_{2v}) and a tetragonal (D_{2d}) (or lower) symmetry has been assigned to the neutral Au center,[6] Au^0. However, the $2p_{1/2}$ state is a Kramers doublet and thus cannot split by low-symmetry crystal fields which excludes the possibility of a crystal-field split final hole state. The excitation spectra are schematically described by $A^0+h\nu\rightarrow A^-+h^+$, where A^0 and A^- indicate the neutral and negatively charged center, respectively, and h^+ indicates the hole in an excited state. We have so far only considered the excited hole but the A^- final core states may very well have an energy-level structure consisting of two nearby states. The interaction between the excited hole and the core states are expected to be small since the two sub systems have very different localization at the impurity site. Assuming that both core states can be reached in the hole transition to the $2P_{1/2}$ state a doublet structure is then expected to be observed even though the hole is excited to an orbital singlet. Such shake-up effects have been observed for, e.g., the neutral interstitial iron center in silicon[10] for which four superimposed shallow-donor spectra were observed. This explanation seems, however, to be very unlikely since the very same doublet structure would then be expected to be observed for all lines, e.g., for the $P_{3/2}$ lines. We conclude this section by noting that all explanations involving excitations to the $2P_{1/2}$ final state seems to be possible to exclude.

In order to identify the origin for the $1S_{3/2}(\Gamma_8)+\Gamma$ line and its replica, we have to find two nearby states being resonant with the $P_{3/2}$ valence-band continuum. In this paper uniaxial-stress measurements on the Au and Pt lines have been carried out. For both centers a similar stress-splitting pattern is observed but with important impurity-dependent differences. It will be shown that the doublet most probably is due to transitions to the $1S_{3/2}(\Gamma_8)$ Coulomb state plus a zone-center phonon coupled to the $P_{3/2}$ valence-band continuum, i.e., a phonon-assisted Fano resonance. The doublet line shape is due to the crystal-field splitting of the $1S_{3/2}(\Gamma_8)$ discrete state. Reorientations effects are observed for both centers in agreement with previous results.[11,12]

II. EXPERIMENTAL DETAILS

The samples were lapped, polished, and etched (HF $+H_2O$) and Pt and Au diffused samples were prepared by sputtering Au or Pt onto 14 Ω cm p-type (boron) floating-zone silicon. The samples were introduced into quartz ampoules filled with argon of about 300 mbar and sealed off. The Pt samples were heat treated at 1260 °C for 1–7 days and the Au samples for 16 h. All samples were quenched to room temperature in ethylene glycol and once again lapped and polished for good optical surfaces. For the PC samples Ohmic contacts were prepared by rubbing Ga-Al onto parts of the surfaces. All spectra were obtained with a BOMEM DA3.02 Fourier-transform infrared spectrometer (FTIR). The sample temperature was in all cases about 10 K. Artificial reference spectra were produced to improve the transparency by suppressing dominating but slowly varying spectral structures.

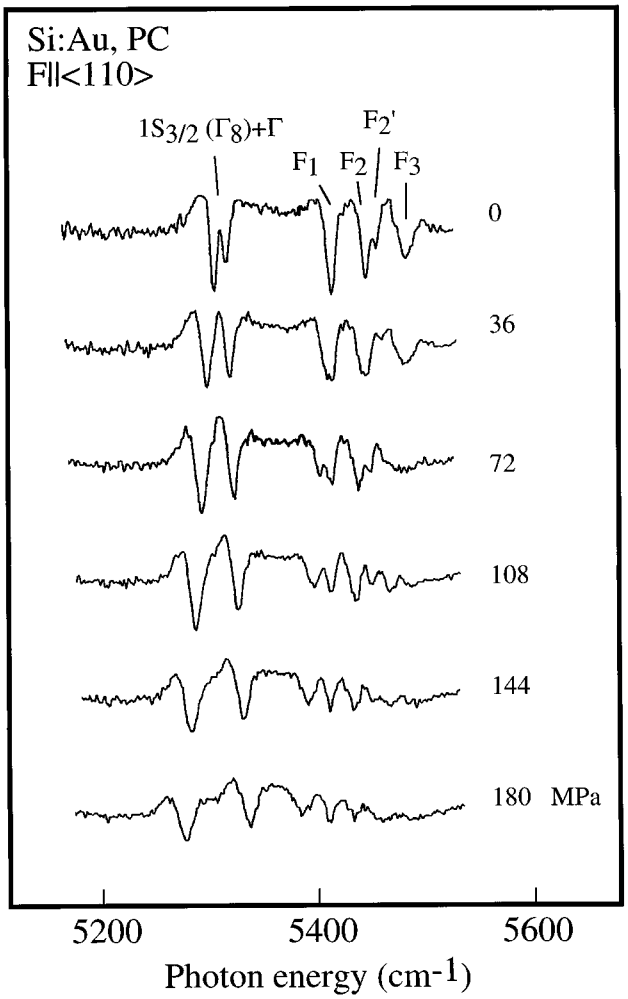

FIG. 2. Si:Au PC spectra obtained for different stress in the ⟨110⟩ direction.

III. EXPERIMENTAL RESULTS AND DISCUSSION

In Fig. 2 PC spectra for the Au acceptor for different stress in the ⟨110⟩ direction are presented. As is readily seen the stress components of the $1S_{3/2}(\Gamma_8)+\Gamma$ lines are well resolved and of similar quality were obtained for the other stress directions as well for the Pt center. For both centers, the stress splitting of the $1S_{3/2}(\Gamma_8)+\Gamma$ lines have been studied by both PC and transmission measurements. The results obtained from the two different techniques are, within experimental errors, identical but as is seen in Fig. 1, the en-

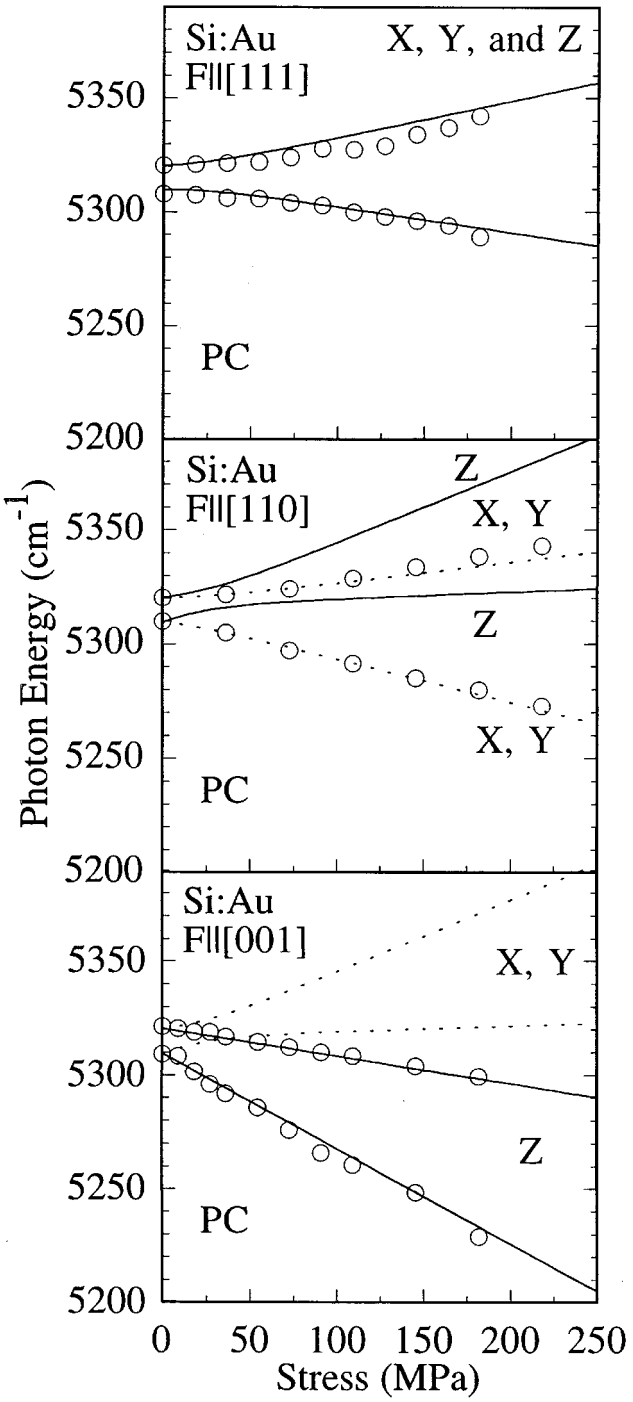

FIG. 3. The uniaxial-stress splitting of the $1S_{3/2}(\Gamma_8)+\Gamma$ Au line for $F||[001]$, [110], and [111]. The spectra have been measured by photoconductivity. X, Y, and Z indicate the orientation of the C_2 axis for individual D_{2d} distorted centers.

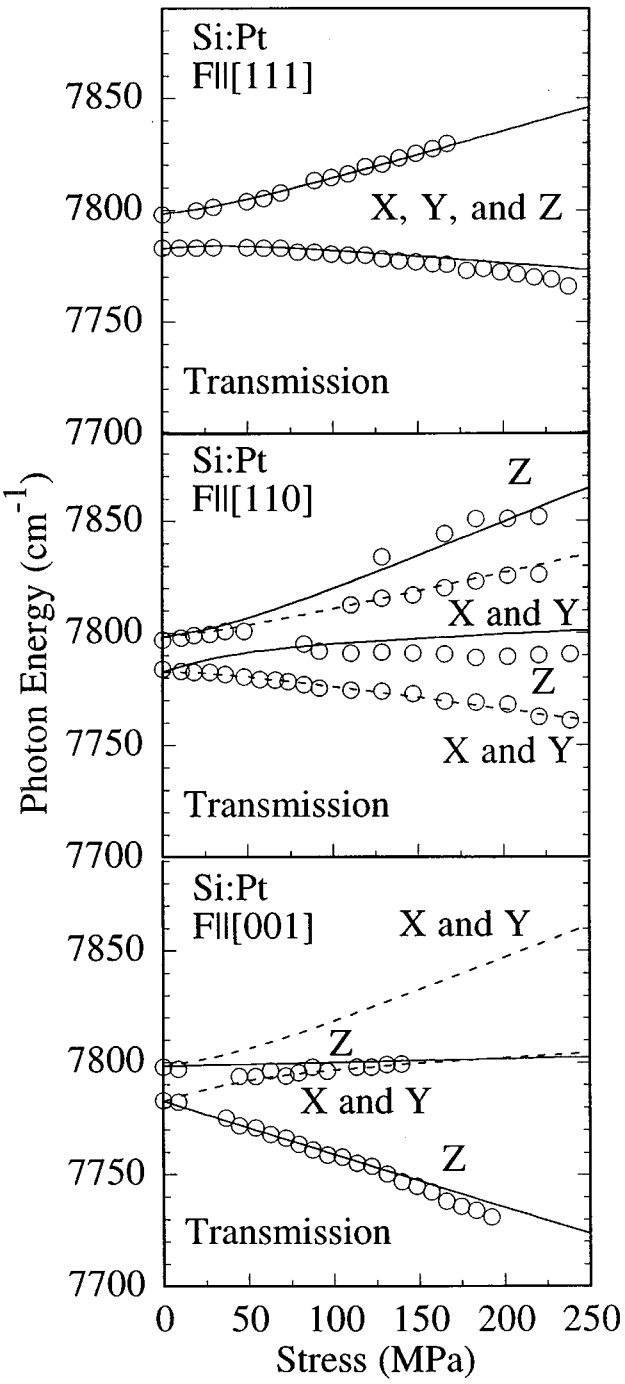

FIG. 4. The uniaxial-stress splitting of the $1S_{3/2}(\Gamma_8)+\Gamma$ Pt line for $F||[001]$, [110], and [111]. The spectra have been measured by transmission. X, Y, and Z indicate the orientation of the C_2 axis for individual D_{2d} distorted centers.

ergy positions of the spectral features, e.g., the minima are not observed at the same energy positions when viewed in PC and transmission. These observations are in agreement with previous results[7] and in order to compare PC and transmission results the corresponding spectra therefore have to be shifted in energy so that, e.g., the minima coincide. In Figs. 3 and 4, the uniaxial-stress results for the Au and Pt $1S_{3/2}(\Gamma_8)+\Gamma$ lines are presented, respectively. the stress splitting was measured with the stress in the [001], [110], and [111] directions. The full and dashed lines show our calculated splitting behavior (see further below). In order to show that the stress-splitting pattern equally well can be studied in both PC and transmission, the Au results were obtained by PC measurements whereas the results for Pt were obtained by transmission measurements. In the case of the Au center, the two partners in the doublet shift differently with stress but no splitting, i.e., no additional components were observed. A clear splitting behavior was, however, detected for Pt center for which four lines were clearly resolved

TABLE I. The splitting due to orientational degeneracy for a D_{2d} center.

Orientation	$\mathbf{F}\|\|[001]$	$\mathbf{F}\|\|[110]$	$\mathbf{F}\|\|[111]$
Z	A_1	A_2	$\frac{1}{2}(A_1+2A_2)$
X and Y	A_2	$\frac{1}{2}(A_1+A_2)$	$\frac{1}{2}(A_1+2A_2)$

for stresses above about 100 MPa for stress parallel to [110]. In spite of this difference the overall stress response is similar for the two centers. As is seen in Figs. 3 and 4, the splitting expected for centers orientated differently with respect to the stress axis have been indicated by X, Y, and Z. The X, Y, and Z centers are defined by their C_2 axis orientated in the [100], [010], and [001] directions, respectively. An excitation line at a tetragonal center is expected to split into 0, 2, and 2 components for stress in the [111], [110], and [001] directions, respectively, since centers orientated differently will experience different stress shifts. This splitting of the orientational degeneracy[13] is described by two parameters A_1 and A_2 and the shifts for different stress directions are presented in Table I. The splitting of an electronic degenerate state may show up as an additional pattern superimposed onto the orientational splitting pattern.

We model the stress splitting by assuming that the transitions originate from a Kramers doublet to a Γ_8 state split by the D_{2d} crystal field although it is well known that the Pt^- center has a C_{2v} symmetry but a dominating D_{2d} distortion. The stress-Hamiltonian matrix $\mathbf{H}_{\mathrm{Stress}}$ become[14]

$$\mathbf{H}_{\mathrm{Stress}}=b\left(\varepsilon_{xx}\left(\mathbf{J}_x^2-\frac{1}{3}J^2\right)+\varepsilon_{yy}\left(\mathbf{J}_y^2-\frac{1}{3}J^2\right)+\varepsilon_{zz}\left(\mathbf{J}_z^2-\frac{1}{3}J^2\right)\right)+\frac{2d}{\sqrt{3}}\times(\varepsilon_{xy}\mathbf{V}_{xy}+\varepsilon_{yz}\mathbf{V}_{yz}+\varepsilon_{zx}\mathbf{V}_{zx}), \quad (1)$$

where $\mathbf{V}_{xy}=1/2\{\mathbf{J}_x\mathbf{J}_y+\mathbf{J}_y\mathbf{J}_x\}$, $\mathbf{V}_{yz}=1/2\{\mathbf{J}_y\mathbf{J}_z+\mathbf{J}_z\mathbf{J}_y\}$, and $\mathbf{V}_{zx}=1/2\{\mathbf{J}_z\mathbf{J}_x+\mathbf{J}_x\mathbf{J}_z\}$. Note that the hydrostatic shift is excluded in Eq. (1) but will be included via the parameters A_1 and A_2. ε_{ij} are components of the strain tensor and $\mathbf{J}_i$ ($i=x$, y, and z) are the angular-momentum matrices for an atomic $J=\frac{3}{2}$ state derived from a $s=\frac{1}{2}$ p state. The values used for the compliance tensor components[15] are $s_{11}=7.617\times10^{-6}$, $s_{12}=-2.127\times10^{-6}$, and $s_{44}=1.246\times10^{-5}$ MPa^{-1}. The parameters b and d are deformation potentials and the stress is defined to be negative for compressional stress. The zero-stress splitting of the Γ_8 state in the D_{2d} crystal field is modeled by effective operators $\mathbf{H}_X$, $\mathbf{H}_Y$, and $\mathbf{H}_Z$, for X, Y, and Z oriented centers, respectively,

$$\mathbf{H}_X=S\cdot(2\mathbf{J}_x^2-\mathbf{J}_y^2-\mathbf{J}_z^2),\quad \mathbf{H}_Y=S\cdot(2\mathbf{J}_y^2-\mathbf{J}_z^2-\mathbf{J}_x^2),\ \text{and}$$

$$\mathbf{H}_Z=S\cdot(2\mathbf{J}_z^2-\mathbf{J}_x^2-\mathbf{J}_y^2), \quad (2)$$

where S is the strength of the distortion and determines the zero-stress splitting for the Γ_8 state. The Hamiltonians have been numerically diagonalized simultaneously and the results are presented in Figs. 3 and 4 and the parameters used are presented in Table II.

TABLE II. The parameters used in the stress-splitting calculations for the Au and Pt centers. The deformation potentials b and d for the boron $1S_{3/2}(\Gamma_8)$ ground state (Ref. 16) is presented for comparison. See text for details.

Center	b (eV)	d (eV)	A_1 (cm^{-1}/MPa)	A_2 (cm^{-1}/MPa)	S (cm^{-1})
Au	−1.9	−4.9	−0.27	0.17	1.8
Pt	−1.6	−4.9	−0.11	0.17	2.6
B	−1.61	−4.5			

By taking both the electronic and orientational degeneracies into account we expect to observe 4, 4, and 2 lines for stress in the [001], [110], and [111] directions, respectively. However, only two lines are detected for all three stress directions for the Au center. In the case of Pt the expected number of lines was observed for [110] and [111] directions whereas only two lines are detected for [001] stress. This may be understood by taking reorientation effects into account. It has been shown that the Pt and Au centers[11,12] preferentially aligns along the stress axis for compressional stress. In equilibrium, the centers are randomly distributed among the three different orientations whereas, e.g., for stress in the [001] direction, X and Y centers change their orientation and, accordingly, the number of Z centers increases. For stress in the [110] direction, X and Y centers are preferred and the number of Z centers decreases. Since all centers have the same angle to the stress axis for [111] stress no alignment occurs in this case. As is seen in Fig. 3, a complete preferential stress alignment is observed for the Au center. For the Pt center, a complete alignment is observed for [001] stress whereas all four line components are observed for [110] stress. It should be noted that a third component has been observed for the Au center for [001] stress when the sample was subjected to inhomogeneous stress.

The uniaxial-stress splitting of the $1S_{3/2}(\Gamma_8)$ ground state of several group-III acceptors in silicon has been determined. The deformation potentials b and d for the boron acceptor $1S_{3/2}(\Gamma_8)$ ground state[16] are presented in Table II. As is readily seen the values for the deformation potentials b and d for the Au and Pt $1S_{3/2}(\Gamma_8)+\Gamma$ are very close to those for boron which strongly suggests that the $1S_{3/2}(\Gamma_8)$ state indeed is involved in doublet line.

The experimental results thus strongly indicate that the Au and Pt doublet line is the $1S_{3/2}(\Gamma_8)+\Gamma$ phonon-assisted Fano resonance. This identification thus enables a simple explanation for the differences in observed line shape when viewed in PC and transmission as well as for the doublet structure. The energy position for the Au and Pt $1S_{3/2}(\Gamma_8)$ pure electronic state is determined by subtracting the Γ phonon energy from the experimental energy positions. The energy positions determined in this way are 4796 and 7278 cm^{-1} for the Au and Pt center, respectively, where we have used the mean value for each doublet. In spite of several attempts no excitation lines have been observed at these energies. In the case of, e.g., the chalcogen double donors in silicon similar observations have been made.[7] Phonon-assisted Fano resonances have been detected for these centers involving electronic states for which zero-phonon transitions have not been observed since the zero-phonon

transitions are symmetry forbidden. In the case of the Au and Pt acceptors, however, we have no reason to expect that transitions to the $1S_{3/2}(\Gamma_8)$ electronic state should be strictly forbidden. It must be pointed out, however, that deep-level acceptor spectra are strongly impurity dependent, i.e., they are very sensitive for the electronic properties of the initial state. Both the Au and the Pt acceptor spectra show close similarities with the group-III acceptor spectra whereas the excitation spectrum for, e.g., the interstitial Mn impurity in silicon[17] is dominated by transitions to $nS_{3/2}(\Gamma_8)$ shallow-acceptor states and thus shows no similarity neither with group-III nor with the Au and Pt spectra. We therefore must conclude that the ''missing'' Au and Pt $1S_{3/2}(\Gamma_8)$ zero-phonon line is due to the detailed electronic properties of the centers ground state.

The binding energies for the Au and Pt acceptors have been deduced in previous optical studies[2,3] and are about 5021.0 cm^{-1} (622.6 meV) and 7511.1 cm^{-1} (931.3 meV), respectively. The $1S_{3/2}(\Gamma_8)$ binding energy becomes 225 cm^{-1} (27.9 meV) and 233.1 cm^{-1} (28.9 meV) for Au and Pt, respectively. These energies are considerably smaller than the binding energies found for the group-III acceptors in silicon. An important difference between deep and shallow centers is that the ground state has a very different origin. For true shallow centers, the acceptor ground state is the $1S_{3/2}(\Gamma_8)$ Coulomb state which possibly is perturbed by central-cell and screening effects whereas for deep centers the ground state is bound by the localized potential. The deep localized state may give rise to a repulsive potential due to orthogonalization effects as have been observed for the interstitial Li donor[18] and for the Pt T-lines[19] in silicon. Such effects may be the cause for the decreased binding energy observed for the $1S_{3/2}$ state.

The $2p'$ line final state for group-III acceptors has been show to be a Kramers doublet (Γ_6). Theoretical calculations[20] have established that there is a Γ_8 state close to the Γ_6 state and that the energy separation is about 0.89 cm^{-1} (0.11 meV). The energy split of the $1S_{3/2}(\Gamma_8)+\Gamma$ Au and Pt line is considerably larger and the possibility that the doublet line is caused by excitation to both the Γ_8 and the Γ_6 state seems very unprobable. Furthermore, in this case the problem of why the $3p'$ line is not observed remains.

IV. CONCLUSIONS

The Pt and Au doublet lines previously identified as the $2p'$ lines have, from the uniaxial-stress study, been identified as transitions to the $1S_{3/2}(\Gamma_8)+\Gamma$ phonon-assisted Fano resonance. The doublet structure is due to a crystal-field splitting due to lower than tetrahedral symmetry of both centers.

ACKNOWLEDGMENTS

The authors acknowledge financial support from the Swedish Natural Science Research Foundation (NFR) and the Swedish Research Council for Engineering Sciences (TFR).

[1] G. Armelles, J. Barrau, M. Brosseau, B. Pajot, and C. Naud, Solid State Commun. **56**, 303 (1985).
[2] M. Kleverman, J. Olajos, and H. G. Grimmeiss, Phys. Rev. B **35**, 4093 (1987).
[3] M. Kleverman, J. Olajos, and H. G. Grimmeiss, Phys. Rev. B **37**, 2613 (1988).
[4] J. W. Peterson and J. Nielsen, Appl. Phys. Lett. **56**, 1122 (1990).
[5] H. H. Woodbury and G. W. Ludwig, Phys. Rev. **126**, 466 (1962).
[6] G. D. Watkins, M. Kleverman, A. Thilderkvist, and H. G. Grimmeiss, Phys. Rev. Lett. **67**, 1149 (1991).
[7] E. Janzén, G. Grossmann, R. Stedman, and H. G. Grimmeiss, Phys. Rev. B **31**, 8000 (1985).
[8] M. Kleverman, G. Grossmann, J. Olajos, and H. G. Grimmeiss (unpublished).
[9] A. K. Ramdas and S. Rodriguez, Rep. Prog. Phys. **44**, 1297 (1981).
[10] J. Olajos, B. Bech Nielsen, M. Kleverman, P. Omling, P. Emanuelsson, and H. G. Grimmeiss, Appl. Phys. Lett. **53**, 2507 (1988).
[11] R. F. Milligan, F. G. Anderson, and G. D. Watkins, Phys. Rev. B **29**, 2819 (1974).
[12] M. Kleverman, A. Thilderkvist, and G. D. Watkins (unpublished).
[13] A. A. Kaplyanskii, Opt. Spectrosc. **16**, 329 (1964).
[14] E. P. Kartheuser, S. Rodriquez, and P. Fisher, Phys. Status Solidi B **64**, 11 (1974).
[15] J. J. Hall, Phys. Rev. **161**, 756 (1967).
[16] H. R. Chandrasekhar, P. Fisher, A. K. Ramdas, and S. Rodriquez, Phys. Rev. B **8**, 3836 (1973).
[17] M. Kleverman, A. Thilderkvist, G. Grossmann, and H. G. Grimmeiss, *Proceedings of the 16th International Conference on Defects in Semiconductors, Bethlehem, 1991* [Mater. Sci. Forum **83–87**, 125 (1992)].
[18] H. Nara and A. Morita, J. Phys. Soc. Jpn. **23**, 831 (1967).
[19] J. Olajos, M. Kleverman, and H. G. Grimmeiss, Phys. Rev. B **40**, 6196 (1989).
[20] R. Buczko and F. Bassani (unpublished).